ACS APPLIED ELECTRONIC MATERIALS

Article

Cite This: ACS Appl. Electron. Mater. 2019, 1, 179−188

pubs.acs.org/acsaelm

Doping Dependence of the Second Magnetization Peak, Critical Current Density, and Pinning Mechanism in $BaFe_{2-x}Ni_xAs_2$ Pnictide Superconductors

Shyam Sundar,*[,†] Said Salem-Sugui, Jr.,[†] Edmund Lovell,[‡] Alexander Vanstone,[‡] Lesley F. Cohen,[‡] Dongliang Gong,[§] Rui Zhang,[∥] Xingye Lu,[⊥] Huiqian Luo,[§] and Luis Ghivelder[†]

[†]Instituto de Fisica, Universidade Federal do Rio de Janeiro, 21941-972 Rio de Janeiro, RJ, Brazil

[‡]The Blackett Laboratory, Physics Department, Imperial College London, London SW7 2AZ, United Kingdom

[§]Beijing National Laboratory for Condensed Matter Physics, Institute of Physics, Chinese Academy of Sciences, Beijing 100190, People's Republic of China

[∥]Department of Physics and Astronomy, Rice University, Houston, Texas 77005, United States

[⊥]Center for Advanced Quantum Studies and Department of Physics, Beijing Normal University, Beijing 100875, People's Republic of China

ABSTRACT: A series of high quality $BaFe_{2-x}Ni_xAs_2$ pnictide superconductors were investigated using magnetic relaxation and isothermal magnetic measurements to study the second magnetization peak (SMP) and critical current behavior in the Ni-doped 122 family. The temperature dependence of the magnetic relaxation rate suggests a pinning crossover, whereas its magnetic field dependence hints at a vortex-lattice structural phase transition. The activation energy (U) estimated using the magnetic relaxation data was analyzed in detail for slightly underdoped, slightly overdoped, and an overdoped sample, using Maley's method and collective creep theory. Our results confirm that the SMP in these samples is due to the collective (elastic) to plastic creep crossover as has been observed for the other members of the 122-family. In addition, we also investigated the doping dependence of the critical current density (J_c) and the vortex-pinning behavior in these compounds. The observed J_c is higher than the threshold limit (10^5 A/cm^2) considered for the technological potential and even greater than 1 MA/cm^2 for the slightly underdoped Ni content, $x = 0.092$ sample. The pinning characteristics were analyzed in terms of the models developed by Dew-Hughes and Griessen et al., which suggest the dominant role of δl-type pinning.

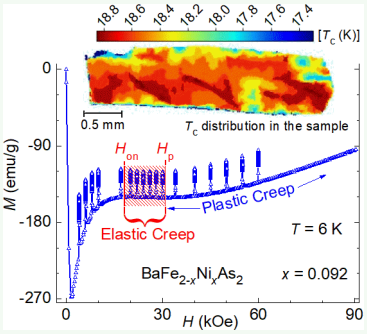

KEYWORDS: *pnictide superconductor, second magnetization peak (SMP), magnetic relaxation, vortex pinning, vortex creep, critical current density, single crystal*

INTRODUCTION

The study of vortex dynamics in type II superconductors gained the interest of experimentalists and theoreticians as soon as the creep phenomenon in magnetization was observed in conventional low-T_c systems.[1−3] From a technological point of view, the creep behavior in magnetization is directly related to a creep in the critical current, showing the importance to understand the vortex-pinning mechanism. Later, the study of vortex dynamics gained attention in the late 1980s with the discovery of the high-T_c cuprates, which show an intrinsic giant thermally activated magnetic relaxation[4] as well as the so-called second magnetization peak (SMP) effect in the isothermal magnetization curves which renders a peak in the critical currents,[5−8] as also observed in the low-T_c superconductors, such as Nb.[9] More recently (2008), the study of vortex dynamics regained the attention of the scientific community due to the discovery of the iron pnictide and iron selenide superconductors[10−13] with a moderately high T_c (from 20 up to 56 K),[14] large upper critical fields, H_{c2},[15,16] small anisotropy,[17−19] and better intergrain connectivity than the cuprates.[20,21] These salient features of iron pnictide superconductors are potentially suitable for application purposes.[22] Besides, pnictides are known as multiband superconductors, which may play a role in the pinning of vortices through the interband and intraband electron scatterings.[23] Since then, vortex dynamics studies were performed on different pnictides compounds discovered over the years,[13,24−31] and most of them are devoted to the study of the mechanism responsible for the appearance of SMP in isothermal magnetization curves. Contrary to the cuprates, where the SMP is mostly observed only for $H\|c$-axis, in Fe pnictides, due to the low anisotropy, it is observed for both $H\|c$-axis and $H\|ab$-planes. A rich variety of mechanisms were proposed as responsible for the SMP in different iron pnictide superconductors, such as crossover from

Received: October 18, 2018
Accepted: January 21, 2019
Published: January 21, 2019

DOI: 10.1021/acsaelm.8b00014
ACS Appl. Electron. Mater. 2019, 1, 179−188

elastic to plastic,[30,32,33] order−disorder transition,[27,34] and vortex−lattice phase transitions.[25,35] However, the mechanism responsible for SMP in Ni-doped $BaFe_2As_2$ pnictide superconductors is as yet unresolved.[29,36,37] Interestingly, in iron pnictide superconductors, it has been observed that the existence of the SMP is doping-dependent.[31,38]

This motivated us to investigate the vortex dynamics in a series of high quality $BaFe_{2-x}Ni_xAs_2$ (x = 0.092, 0.108, 0.12, 0.15, 0.18, and 0.065) pnictide superconductors. In addition to the detailed study of the SMP in different Ni-content samples, a complementary study of the critical current density and the pinning behavior is also performed on all samples using magnetic relaxation and isothermal magnetic measurements. A detailed analysis of the magnetic relaxation data using Maley's method[39] and collective pinning theory[40] unambiguously shows that the SMP in Ni-doped $BaFe_2As_2$ compounds is due to the collective (elastic) to plastic creep crossover, which might be accompanied by a vortex-lattice structural phase transition, similar to the Co-doped $BaFe_2As_2$ superconductor. The critical current density is found to be higher than the threshold limit (>10^5 A/cm^2) considered for technological applications. The doping dependence of critical current density, $J_c(x)$, does not follow the variation of superconducting transition temperature with Ni content, $T_c(x)$, and shows a spike feature at x = 0.092. The dominant pinning in these crystals is found to be related to the variation of the charge carrier mean free path, generally known as δl-type pinning.

EXPERIMENTAL DETAILS

A detailed study of a series of six $BaFe_{2-x}Ni_xAs_2$ pnictide superconductors is performed. Details of the crystal growth are described in ref 41. Large crystals were cut into small pieces with typical dimensions of 2.5 mm × 1 mm × 0.15 mm using a clean scalpel, and the samples with sharpest superconducting transition were chosen for each concentration to study. Surface maps of T_c measured for two chosen samples (x = 0.092 and 0.108) using a scanning Hall probe magnetometer with a 5 μm × μm active area of the Hall sensor (2.5 μm thick InSb epilayer on undoped GaAs substrate)[42] are shown in Figure 1. A 4 T split coil superconducting magnet and a continuous flow helium cryostat (Oxford Instruments Ltd.) were used to perform the measurements. The imaging was performed by applying 1 mT magnetic field (parallel to the c-axis) in the zero field cooled state below T_c and mapping the Meissner current profile across the crystal. At low temperature the screen current perfectly follows the edge of the sample. The mapping shows that the T_c distribution within the crystals studied is rather uniform and of high quality. The screening diminishes from the edges toward the center of the sample as expected within the measured transition width, consistent with the global magnetometry $M(T)$ data. Magnetization measurements were performed using a vibrating sample magnetometer (VSM, Quantum Design, USA), where the sample was mounted between the two quartz cylinders in a brass sample holder. The temperature and magnetic field dependence of the magnetization, $M(T)$ and $M(H)$, and the magnetic relaxations, $M(t)$, were measured for $H\|c$-axis down to 2 K and up to 9 T magnetic field in the zero field cooled (zfc) mode. To investigate the behavior of SMP in the samples, each $M(t)$ was measured over a period of ∼90 min at fixed magnetic field in the increasing cycle of the isothermal $M(H)$ curves.

RESULTS AND DISCUSSION

Figure 2 shows the temperature dependence of magnetization, $M(T)$, measured for all samples in zfc mode with H = 1 mT. The sharp drop in the magnetization for the diamagnetic signal is considered as the onset of the superconducting transition (T_c), shown with an arrow in Figure 2. The sharp

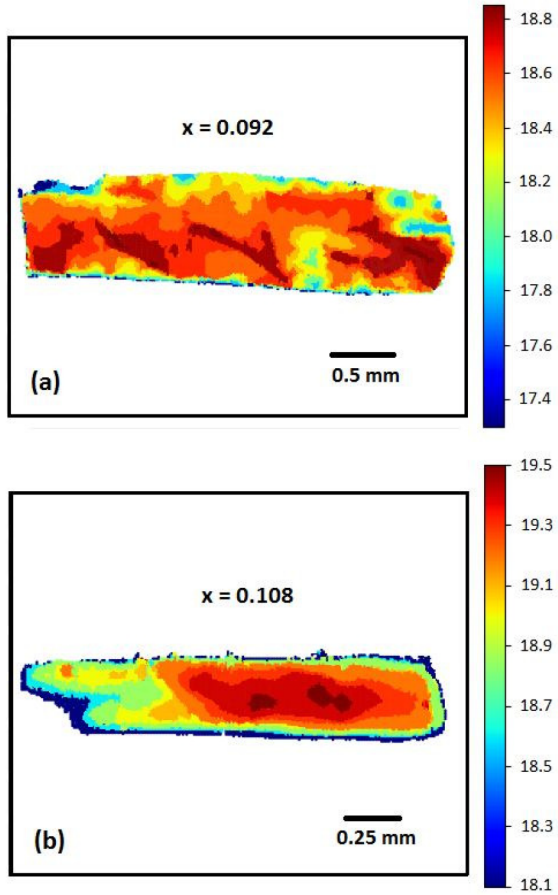

Figure 1. Distribution of the superconducting transition temperature (T_c) in (a) x = 0.092 and (b) x = 0.108 samples, measured using a scanning Hall probe magnetometer. Variation of the T_c over the scanned surface is identified by labels in each panel. Both images show the good quality of the samples.

superconducting transition is an indication of the good quality of the samples, and the obtained T_c values are in fair agreement with the available literature.[41,43] For $BaFe_{2-x}Ni_xAs_2$ superconductors, the optimal doping is x = 0.1 with T_c = 20.1 K.[41,43] In this study, the maximum T_c = 19.5 K is observed for x = 0.108, which is slightly overdoped, and for more overdoped samples T_c decreases. Similarly, x = 0.092 is slightly underdoped and shows the T_c = 18.8 K, which further decreases for more underdoped samples.

Magnetic Relaxation and the Second Magnetization Peak (SMP). Figure 3 shows selected isothermal $M(H)$ curves measured in zfc mode at various temperatures below T_c down to 2 K. The symmetric behavior of isothermal $M(H)$ suggests the dominant role of bulk pinning for all samples under study. A clear signature of the SMP is observed for each doping content, except for the highly underdoped, x = 0.065 sample. The absence of SMP in the x = 0.065 sample is might be due to the static antiferromagnetic long-range order, which exists in low doped $BaFe_{2-x}Ni_xAs_2$.[44] The onset and the peak position of the SMP are defined as H_{on} and H_p, respectively. The magnetic hysteresis in the field increasing and field decreasing cycles of the $M(H)$ vanishes at higher fields, defined as the irreversibility field, H_{irr}. Interestingly, in slightly underdoped composition, x = 0.092, the SMP is smeared out below 5 K. This is called faded SMP, as seen in Figure 4a. To confirm this anomaly, we repeated the measurements on another crystal

DOI: 10.1021/acsaelm.8b00014
ACS Appl. Electron. Mater. 2019, 1, 179−188

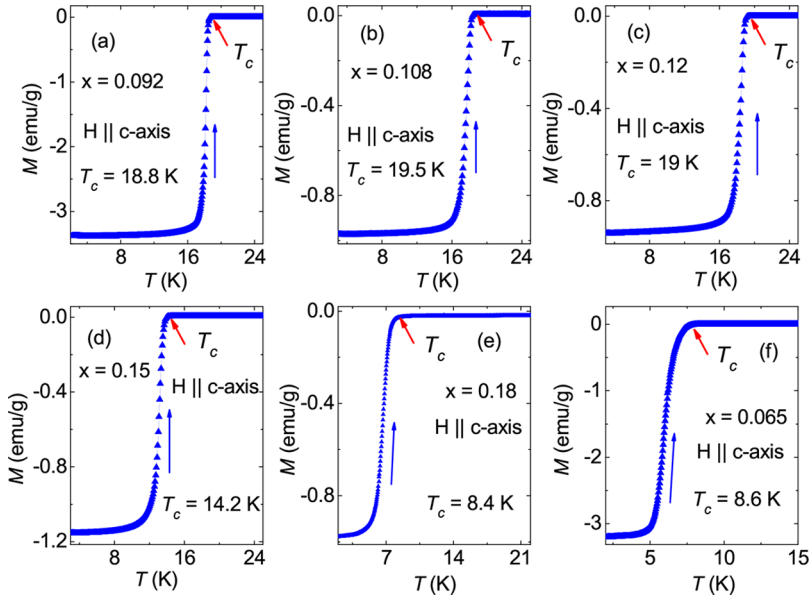

Figure 2. (a–f) Temperature dependence of magnetization, $M(T)$, of $BaFe_{2-x}Ni_xAs_2$ pnictide superconductors measured in zfc mode with H = 1 mT.

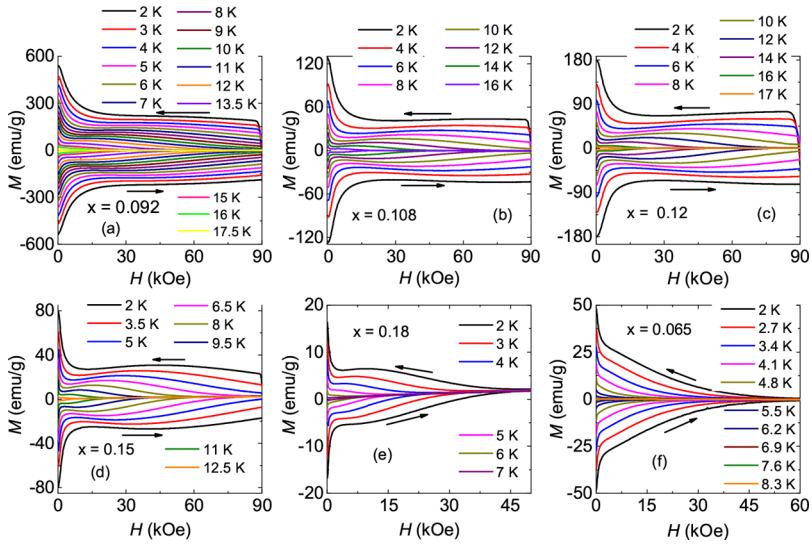

Figure 3. Isothermal magnetic field dependence of magnetization, $M(H)$, for x = (a) 0.092, (b) 0.108, (c) 0.12, (d) 0.15, (e) 0.18, and (f) 0.065 $BaFe_{2-x}Ni_xAs_2$ pnictide superconductors, in field increasing and field decreasing cycle. Each sample show the second magnetization peak feature below T_c, except the highly underdoped, x = 0.065 sample.

with same x content (same T_c) and observed the same behavior. Similar anamolous behavior has also been observed in the Bi–Sr–Ca–Cu–O single crystal, where the SMP was only observed in a temperature range 20–40 K below T_c.[45,46] In contrast to that, a recent study of $Ba_{0.75}K_{0.25}Fe_2As_2$ superconductor showed the SMP only at temperatures below $T_c/2$ and vanished at higher temperatures.[30]

To investigate the origin of the SMP in $BaFe_{2-x}Ni_xAs_2$, with x = 0.092 (slightly underdoped), x = 0.108 (slightly overdoped), and x = 0.15 (overdoped) superconductors, we performed magnetic relaxation, $M(t)$, at selected temperature and magnetic field values for ~90 min in the lower branch of the $M(H)$ curves. In Figure 4b, magnetic relaxation results are shown for x = 0.092 at T = 5 K. A circle in Figure 4b highlights the initial 15 s of relaxation, which corresponds to ~40% of the total magnetic relaxation in a period of 90 min of measurement. This feature is observed in all samples under investigation and is also found in a recent study of $Ba_{0.75}K_{0.25}Fe_2As_2$.[30] All magnetic relaxations follow the usual logarithmic behavior with time, $|M| \sim \log(t)$, and the plots of $\ln|M|$ vs $\ln t$ allowed us to obtain the relaxation rate, $R = -\mathrm{d} \ln M/\mathrm{d} \ln t$.

Figure 5 shows the relaxation rate as a function of magnetic field for samples with x = 0.092, 0.108, 0.15, and 0.065. For each Ni content, a peak in $R(H)$ associated with the SMP is observed in each curve. A similar feature has also been observed in the SMP study of Co-doped $BaFe_2As_2$ and explained in terms of the vortex-lattice structural phase transition.[25,32] It is worth mentioning the absence of a peak in $R(H)$ for the x = 0.065 sample, which does not show the SMP.

DOI: 10.1021/acsaelm.8b00014
ACS Appl. Electron. Mater. 2019, 1, 179–188

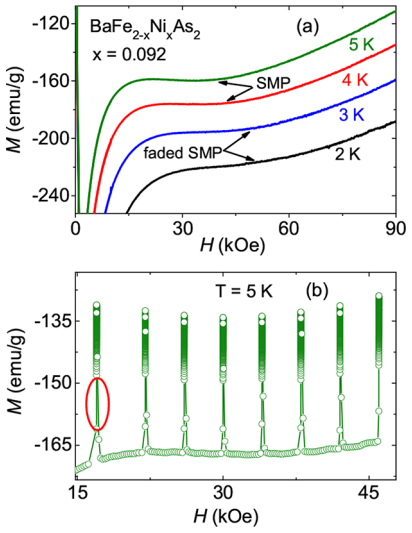

Figure 4. (a) Isothermal $M(H)$ for $BaFe_{2-x}Ni_xAs_2$, x = 0.092 sample at some selected temperatures, where below T = 4 K, the SMP feature smeared out. (b) Isothermal $M(H)$ at T = 5 K with magnetic relaxation data measured for selected magnetic fields. The circle highlights the rapid magnetic relaxations for the first 15 s.

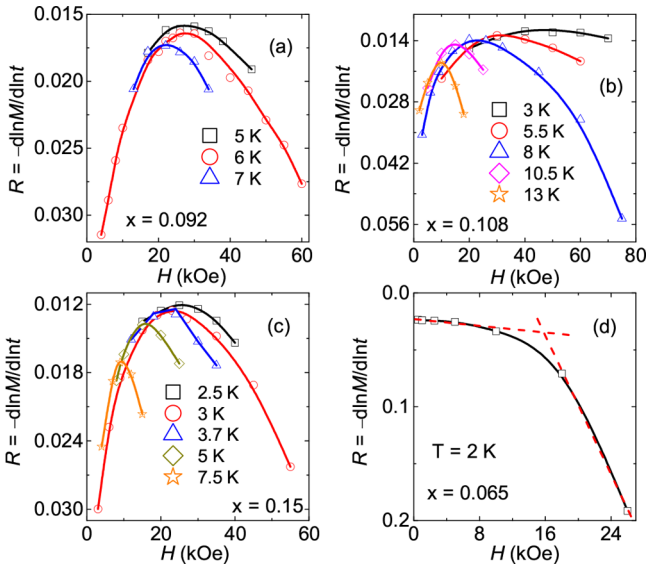

Figure 5. Magnetic field dependence of relaxation rate, $R = -\mathrm{d}\ln M/\mathrm{d}\ln t$, for $BaFe_{2-x}Ni_xAs_2$: x = (a) 0.092, (b) 0.108, (c) 0.15, and (d) 0.065 samples. Each sample shows the clear peak structure in every isothermal $R(H)$, except the x = 0.065 sample, which also does not show the second magnetization peak feature.

The characteristic magnetic fields associated with the SMP, H_{on}, H_p, H_{irr}, and H_m, are shown in Figure 6 with H_{on} and H_p lying far below the H_{irr} line. It should be noted that the behavior of the temperature dependence of H_p is different in x = 0.092 compared to the other samples used in this study. It should also be noted that H_m lies in between the H_{on} and H_p lines as previously observed in the case of Co-doped $BaFe_2As_2$.[25,32] Since the peak position, H_m, in the $H-T$ phase diagram varies with temperature in a similar way as observed for $Ba(Fe_{0.925}Co_{0.075})_2As_2$,[25] we suggest that this behavior might be associated with the vortex-lattice structural phase transition in this study. However, it is argued that such

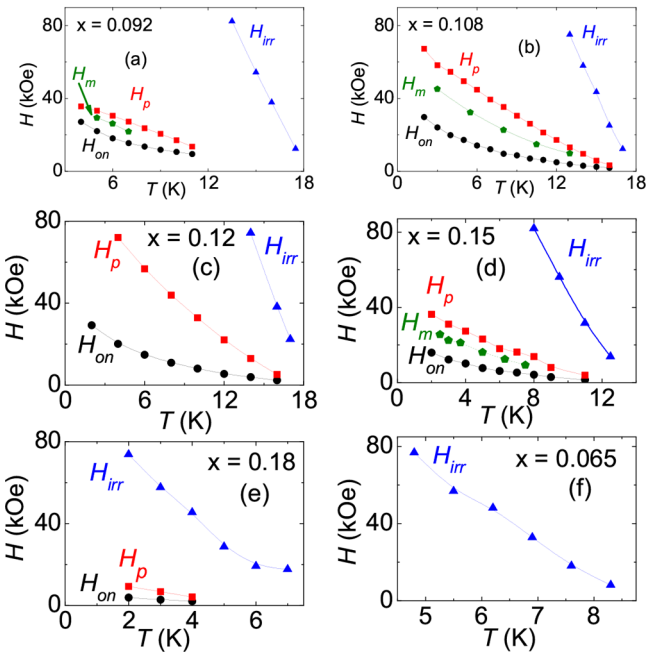

Figure 6. $H-T$ phase diagram for x = (a) 0.092, (b) 0.108, (c) 0.12, (d) 0.15, (e) 0.18, and (f) 0.065 samples. The characteristic fields H_{on}, H_p, H_{irr}, and H_m are well explained in the text.

vortex-lattice structural phase transition may be followed by a crossover in creep behavior.[6,25,32]

Figure 7 shows the temperature dependence of the relaxation rate, $R(T)$, for x = 0.108 and 0.15 measured with

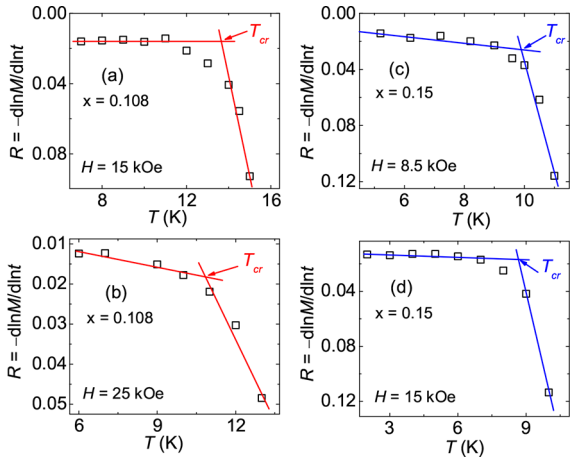

Figure 7. Temperature dependence of relaxation rate, $R = -\mathrm{d}\ln M/\mathrm{d}\ln t$, for $BaFe_{2-x}Ni_xAs_2$: x = (a, b) 0.108 and (c, d) 0.15 samples. Each isofield $R(T)$ shows a crossover in slope, which is defined as T_{cr}. The crossover in the slope suggests the crossover in pinning behavior and is apparently related to the second magnetization peak (H_p) in the sample.

different magnetic fields. Each isofield $R(T)$, for both samples, shows a clear change of slope at T_{cr}. Interestingly, T_{cr} values obtained from Figure 7a–d are well matched with the H_p line in the $H-T$ phase diagram, suggesting that a pinning crossover is responsible for the SMP. A peak behavior observed simultaneously in isofield $R(T)$ and $R(H)$ has been argued as a possibility for a vortex-lattice structural phase transition in different superconductors,[25,35,47] but in the present case the

DOI: 10.1021/acsaelm.8b00014
ACS Appl. Electron. Mater. 2019, 1, 179–188

peak positions of $R(H)$ and $R(T)$ do not match. As we see in Figure 5, each isothermal $R(H)$ shows a peak behavior; however, the isofield $R(T)$ shown in Figure 7a–d only shows a change of slope and does not exhibit a clear peak structure.

We exploited the temperature dependence of the relaxation rate, $R(T)$, to obtain the activation energy ($U^* = T/R$) and plotted it in Figure 8 as a function of the inverse current

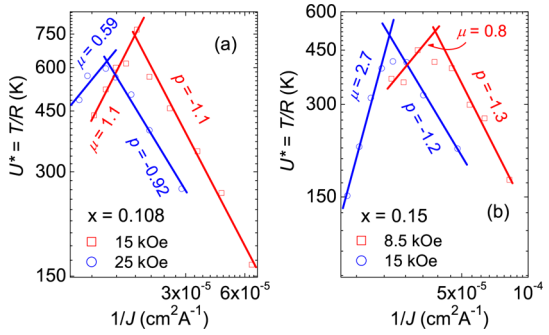

Figure 8. Activation energy ($U^* = T/R$) as a function of the inverse current density ($1/J$) for $BaFe_{2-x}Ni_xAs_2$: x = (a) 0.108 and (b) 0.15 samples. For both samples, the value of the parameters (μ and p) in each curve suggests the elastic to plastic pinning crossover and the crossover point are well matched with the H_p.

density, $1/J$, where J is obtained using Bean's critical state model, as discussed later. A U^* vs $1/J$ plot has been extensively used to investigate the vortex dynamics in pnictide superconductors.[30,32,33,48] To relate the activation energy (U^*) with the critical current density (J_c), we used an expression from the theory of collective flux creep,[40] $U^* = U_0(J_c/J)^{\mu}$, where μ and J_c depend on the dimensionality and size of the flux bundles under consideration.[40] Using this expression, one may obtain the exponent μ by a double-logarithmic plot of U^* vs $1/J$, which is shown in Figures 8a and 8b for x = 0.108 and 0.15 samples, respectively. For a 3-dimensional system, the predicted values of exponent μ are reported as 1/7, 3/2, and 7/9 for single-vortex, small-bundle, and large-bundle regimes, respectively.[40,49] However, the obtained μ values for x = 0.108 are 1.1 and 0.59 for H = 15 and 25 kOe and μ for x = 0.15 are 0.8 and 2.7 for H = 8.5 and 15 kOe, respectively (see Figure 8a,b). These μ values are different than the predicted ones, as found in other studies on several superconductors.[24,27,33,50−52] Similarly, values of the exponent (p) at the higher temperature side (low J) are also found to be different than the predicted value for plastic creep (p = 0.5).[5,32] Although the observed exponents in Figure 8a,b are different than the expected values, the plots of U^* vs $1/J$ in this study suggest a crossover in the pinning mechanism is responsible for SMP.

To confirm a possible pinning crossover, observed in Figures 7 and 8 for $R(T)$ and $U^*(1/J)$ curves, respectively, we plotted the activation energy, U, of the x = 0.092 and 0.15 samples as a function of magnetization, M, by invoking the method developed by Maley et al.[39] (similar results are observed for x = 0.108 but are not shown here). Such methodology has been widely used to investigate the vortex dynamics associated with SMP in different iron pnictide superconductors[30,31,33,38,39,50] and is expressed as

$$U = -T \ln[dM(t)/dt] + CT \quad (1)$$

where C is a constant which depends on the hopping distance of the vortex, the attempt frequency, and the sample size. The activation energy as a function of magnetization is plotted in Figures 9a and 9b for x = 0.0.092 and x = 0.15 samples,

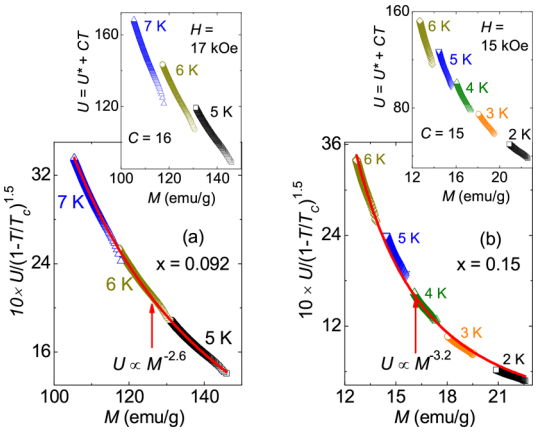

Figure 9. Variation of activation energy (U) scaled with a function, $g(T/T_c) = (1 - T/T_c)^{1.5}$, is plotted as a function of magnetization (M) for $BaFe_{2-x}Ni_xAs_2$: x = (a) 0.092, and (b) 0.15 samples. Each scaled curve follow the power law behavior. The inset of each panel shows $U(M)$ before scaling by the $g(T/T_c)$ function. Similar results are also observed for the x = 0.108 sample (not shown here).

respectively. The insets in Figures 9a,b show the U vs M curves for x = 0.0.092 and 0.15 samples using C = 16, 25, and 15. Similar values have been previously reported.[32,50,53] The U vs M curves for each sample, as shown in the inset figures, do not show a smooth behavior. The curves showing a smooth power law behavior are obtained after dividing U by $g(T/T_c) = (1 - T/T_c)^{1.5}$, as suggested in ref 53 and verified in numerous studies.[30−32,38,50] The smooth curves of $U/(1 - T/T_c)^{1.5}$ vs M are shown in each main panel of Figure 9. The values of the parameter C used in Figure 9 are employed to extract the activation energy from the magnetic relaxation data in different field regimes, such as $H < H_{on}$, $H_{on} < H < H_p$, and $H > H_p$, to investigate the SMP behavior in x = 0.092, 0.108, and 0.15 samples (results for x = 0.108 are not shown here).

To demonstrate the origin of the SMP in a series of $BaFe_{2-x}Ni_xAs_2$, we plotted the activation energy as a function of magnetization, $U(M)$, shown in the inset of each panel of Figure 10. For x = 0.092 and 0.15 samples, the $U(M)$ curves were plotted for T = 6 and 3 K, respectively, in three different magnetic field regimes. These $U(M)$ curves were analyzed in terms of the theory of collective flux creep,[5,40] in which the activation energy is defined as

$$U(B, J) = B^{\nu}J^{-\mu} \approx H^{\nu}M^{-\mu} \quad (2)$$

where the exponents ν and μ depend on the specific pinning regime. According to the collective creep theory, the activation energy (U) increases with the magnetic field (H), and if the activation energy decreases with increasing magnetic field, it is suggestive of plastic creep behavior.[5] Therefore, in eq 2, the positive value of ν suggests a collective creep mechanism and, similarly, a negative value indicates plastic creep.[5,40] To examine the collective (elastic) to plastic creep crossover in the samples, we scaled U with H^{ν} for each sample under investigation in different magnetic field regimes for different values of ν, as shown in Figure 10. The positive and negative values of the exponent ν in $H_{on} < H < H_p$ and $H > H_p$ magnetic field regions for each sample (x = 0.092 and 0.15) clearly demonstrate the collective (elastic) to plastic creep crossover

DOI: 10.1021/acsaelm.8b00014
ACS Appl. Electron. Mater. 2019, 1, 179−188

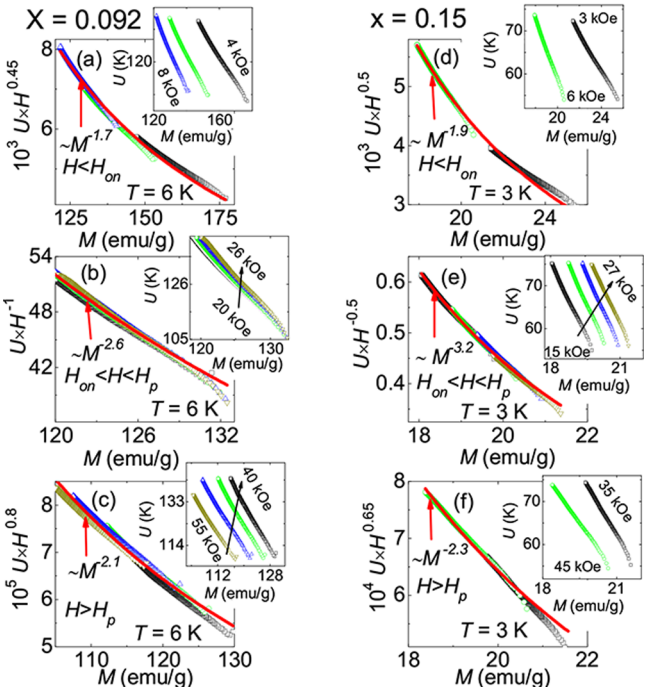

Figure 10. Activation energy (U) scaled using the theory of collective flux creep is plotted as a function of magnetization (M) in panels a–c for x = 0.092 and panels d–f for x = 0.15, in different magnetic field regimes (see text). Each sample shows the collective (elastic) to plastic creep crossover. Each inset shows the U vs M without scaling in different magnetic field regimes. Similar results are also observed for x = 0.108 sample (not shown here).

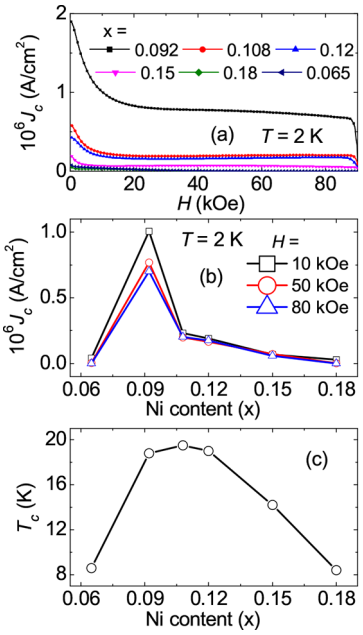

Figure 11. (a) Comparison of the magnetic field dependence of the critical current density, $J_c(H)$, at T = 2 K, between distinct doping (x) contents in $BaFe_{2-x}Ni_xAs_2$ superconductors. (b) Critical current density at T = 2 K plotted as a function of Ni content (x). The maximum in $J_c(x)$ corresponds to x = 0.092. (c) Doping dependence (x) of the superconducting transition temperature (T_c). The peak in $T_c(x)$ corresponds to the x = 0.108; however, the optimal doping for $BaFe_{2-x}Ni_xAs_2$ superconductors is x = 0.1.[41]

as the origin of SMP in $BaFe_{2-x}Ni_xAs_2$. Similarly, elastic to plastic creep crossover is also observed for the x = 0.108 sample, as the origin for SMP, but results are not shown here. In Figures 10a and 10d, the scaling of U vs M curves for $H < H_{on}$ also shows the negative value of ν, which would indicate the unphysical plastic creep nature. However, such behavior is observed in other studies and has been well explained in terms of single vortex pinning (SVP).[5,30,32,33,50] The crossover from SVP to collective creep renders a peak at H_{on}, which is entirely different in nature than the SMP at H_p.

Critical Current Density and Pinning Behavior. The magnetic field dependence of critical current density, $J_c(x)$, at T = 2 K, for each Ni content is shown in Figure 11a. Bean's critical state model[54] is exploited to extract the J_c, using J_c (A cm^{-2}) = $20\Delta M/a(1 - a/3b)$, where ΔM (emu cm^{-3}) is the difference between the upper and lower branches of the isothermal $M(H)$ curves and a and b are the dimensions of a rectangular-shaped sample ($a < b$ in cm) perpendicular to the applied magnetic field direction.[32,55] The critical current density (J_c) in iron-based superconductors is quite important for their potential use in technological applications.[55,56] The maximum, $J_c \approx 2$ MA/cm^2, is observed for the slightly underdoped sample, x = 0.092, in the zero field limit at T = 2 K. On the other hand, for overdoped compounds (x = 0.108, 0.12, and 0.15), J_c is found to be higher than the threshold limit for technological application ($\approx 10^5$ A/cm^2) in the zero magnetic field limit, even at liquid helium temperature (T = 4.2 K). For further Ni doping, x = 0.18, J_c decreases to the 10^4 A/cm^2 order of magnitude. It is found that the J_c corresponding to the optimal doping (x = 0.1)[26,57] is smaller than the slightly underdoped (x = 0.9) regime,[58] as has been also observed in the case of $Ba_{1-x}K_xFe_2As_2$.[55] The J_c values above 10^5 A/cm^2 in overdoped samples and even more than 1 MA/cm^2 in slightly underdoped compound make $BaFe_{2-x}Ni_xAs_2$ a potential candidate for application purposes.[56]

Figure 11b shows the behavior of J_c as a function of Ni content (x) measured at T = 2 K for different magnetic field values. It is interesting to see that $J_c(x)$ shows a spikelike behavior at x = 0.092 for each curve plotted for H = 10, 50, and 80 kOe. Interestingly, the $J_c(x)$ curve shown in Figure 11b is distinctively different than the $T_c(x)$ plot presented in Figure 11c, which shows a broad domelike behavior[17,41] instead of the spikelike peak shown in Figure 11b. Such behavior between $J_c(x)$ and $T_c(x)$ was also seen by Song et al. in $Ba_{1-x}K_xFe_2As_2$.[55]

To investigate the pinning behavior in $BaFe_{2-x}Ni_xAs_2$, we estimate the pinning force density using $F_p = J_c \times H$, where J_c is the critical current density and H is the magnetic field. The normalized pinning force density is plotted as a function of reduced magnetic field ($h = H/H_{irr}$) in Figure 12a–f and is analyzed using the model developed by Dew-Hughes,[59] which has been widely used in many other studies.[33,57,60,61] The magnetic irreversibility field (H_{irr}) is extracted by considering the magnetic field value where $J_c \leq 50$ A/cm^2, below which the J_c decreases to the noise level. The scaling of the normalized pinning force curves shows a single peak for each sample under study. However, a close inspection of the scaled curves for different T shows a slightly poor scaling for x = 0.108, 0.12, and 0.18 samples, with two nearby peaks, as shown with arrows in Figure 12b,c,e. On the other hand, samples with x = 0.092, 0.15, and 0.065 show a good scaling with only one peak (see Figure 12a,d,f). A peak behavior of the scaled curve of pinning force suggests a single dominating pinning behavior, which

DOI: 10.1021/acsaelm.8b00014
ACS Appl. Electron. Mater. 2019, 1, 179–188

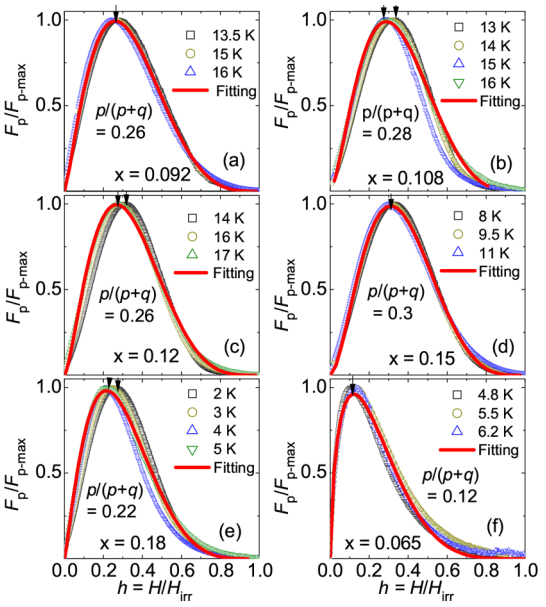

Figure 12. Normalized pinning force density ($F_p/F_{p\text{-max}}$) as a function of reduced magnetic field, $h = H/H_{irr}$ for for x = (a) 0.092, (b) 0.108, (c) 0.12, (d) 0.15, (e) 0.18, and (f) 0.065 samples. For each sample, data collected at different temperatures scaled to a single curve, and the solid line is fit to the scaled curve using $f_p = A(h)^p(1-h)^q$, where the parameters p and q define the pinning characteristics of the sample.

may be described in terms of a mathematical expression, $F_p/F_{p\text{-max}} = A(h)^p(1-h)^q$, where A is a multiplicative factor, $F_{p\text{-max}}$ is the maximum pinning force density at constant temperature, the parameters p and q provide the details about the pinning mechanism, and the peak position is defined by $p/(p+q)$.[60,62] This expression was used to fit the scaled pinning force data shown in Figure 12a–f, where the solid line represents the fitting. The obtained parameters A, p, and q and the peak position $p/(p+q)$ for each sample are presented in Table 1.

Table 1. Parameters Obtained by Fitting the Expression $F_p/F_{p\text{-max}} = A(h)^p(1-h)^q$ to the Experimental Curves $F_p/F_{p\text{-max}}$ vs h

samples	A	p	q	$p/(p+q)$
x = 0.092	17.3	1.3	3.6	0.26
x = 0.108	25.4	1.5	3.8	0.28
x = 0.12	24.5	1.4	4.0	0.26
x = 0.15	35.1	1.7	3.9	0.3
x = 0.18	18.2	1.2	4.4	0.22
x = 0.065	6.4	0.6	4.5	0.12

It is known from the Dew-Hughes model that the high value of the peak position ($h > 0.33$) is an indication of dominant δT_c pinning, and peak position lower than h = 0.33 suggests the dominant role of δl pinning and pointlike pinning centers.[28,59,60,62] Therefore, the peak positions shown in Table 1 indicates the δl pinning behavior for almost all investigated samples. However, for x = 0.065 (highly underdoped), the peak position is found to be 0.12, which is quite smaller than the overdoped and nearly optimally doped samples. This scenario suggests that the pinning behavior in overdoped and underdoped regimes are quite different in nature. It is to be noted that the peak position of the scaled pinning force curves is found at $h \sim 0.3$ in the study of a slightly underdoped x = 0.09 sample.[58] In other studies of optimally doped samples (x = 0.1), the scaled pinning force curves show $h \geq 0.4$,[29,57] which would suggest the δT_c pinning. However, ref 29 suggests the dominance role of δT_c pinning in the sample, whereas ref 57 claims a strong signature of δl-type pinning. As we know, the peak position in the scaled pinning force curves is dependent on the value of irreversibility field, H_{irr}, and on the basis of the criterion to chose the H_{irr}, one may get a smaller or larger value of peak position (h). This shows that a method based on the peak position to describe the pinning mechanism is not robust enough. Therefore, we used the another approach to clear the ambiguity between the δl and δT_c-type pinning in Ni-doped 122 superconductors.

To explore the nature of pinning in a series of $BaFe_{2-x}Ni_xAs_2$ superconductors, we investigate the temperature dependence of J_c at different magnetic fields and used the model developed by Griessen et al.[63] In this model, the pinning due to the spatial variation of the charge carrier mean free path, δl, and the spatial variation of the superconducting transition temperature, δT_c, have been described as $\delta l(J_c(t)/J_c(0) = (1-t^2)^{5/2}(1+t^2)^{-1/2})$ and $\delta T_c(J_c(t)/J_c(0) = (1-t^2)^{7/6}(1+t)^{5/6})$. This model has been widely accepted to investigate the nature of vortex pinning in superconductors.[64,65] Figure 13a–f shows

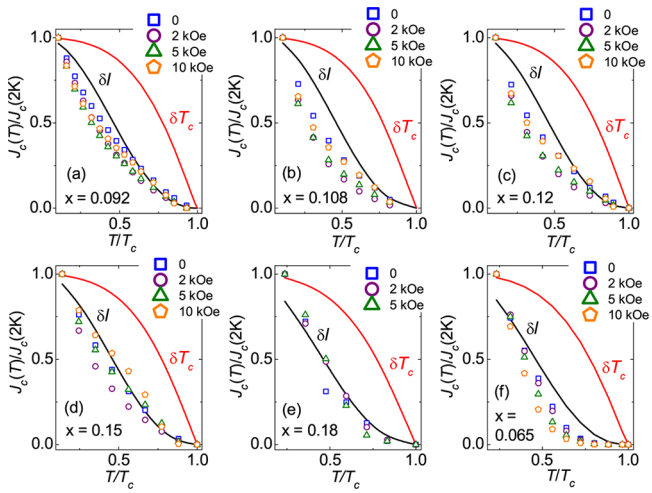

Figure 13. Normalized critical current density, $J_c/J_c(0)$, as a function of reduced temperature, T/T_c for x = (a) 0.092, (b) 0.108, (c) 0.12, (d) 0.15, (e) 0.18, and (f) 0.065 samples. The solid lines present the δl and δT_c pinning models. Each sample shows close resemblance with the δl-type pinning mechanism.

$J_c(T)/J_c(2\text{ K})$ vs T/T_c plots at different constant H and suggests the close resemblance with the δl-type pinning mechanism in all six samples under study. This result is consistent with the observation by Shahbazi et al.[57] Bitter decoration patterns on optimally doped and overdoped $BaFe_{2-x}Ni_xAs_2$ show a highly inhomogeneous including large- and small-scale stripelike vortex patterns[26] preferably due to the dominant role of δl-type pinning.

SUMMARY AND CONCLUSION

In summary, we studied a series of high quality $BaFe_{2-x}Ni_xAs_2$ pnictide superconductors to investigate the doping dependence of the SMP, critical current density, and the pinning characteristics. The SMP feature is observed in all samples except in a highly underdoped one, x = 0.065. Interestingly, for

DOI: 10.1021/acsaelm.8b00014
ACS Appl. Electron. Mater. 2019, 1, 179–188

x = 0.092, the SMP feature is not prominent at low temperatures but is clearly visible above T = 5 K. The temperature dependence of the relaxation rate, $R(T)$, suggests a pinning crossover, whereas its magnetic field dependence, $R(H)$, at different isothermals shows a peak structure. The peak position in $R(H)$, H_{sp}, lies in between the characteristic fields H_p and H_{on} associated with the SMP. In reference to other studies, such behavior is described in terms of the vortex-lattice structural phase transition, which is followed by a pinning crossover. To confirm the pinning crossover, magnetic relaxation data were used to extract the activation energy (U) and were analyzed using Maley's method and collective pinning theory. The analysis unambiguously shows the collective (elastic) to plastic creep crossover as the origin of the SMP in Ni-doped $BaFe_2As_2$ superconductors. Such pinning crossover may be accompanied by a vortex-lattice structural phase transition below H_p. The critical current density (J_c) estimated using Bean's critical state model is found to be larger than the threshold limit (>10^5 A/cm^2) considered for the technological relevance and even exceeds 1 MA/cm^2 for the x = 0.092 sample at low temperatures. However, for highly overdoped (x = 0.18) and underdoped (x = 0.065) samples, the observed J_c is lower than the threshold limit. The pinning behavior in the samples is analyzed by plotting the normalized pinning force density ($F_p/F_{p\text{-}max}$) as a function of reduced magnetic field ($h = H/H_{irr}$), which suggests the pointlike pinning centers in the samples. The plot of reduced temperature (T/T_c) dependence of the normalized critical current density ($J_c(T)/J_c(2\ K)$) suggests that the pinning in the sample is related to the variation of the charge carrier mean free path (δl-type pinning).

AUTHOR INFORMATION

Corresponding Author

*E-mail: shyam.phy@gmail.com (S.S.).

ORCID

Shyam Sundar: 0000-0003-2855-7989

Said Salem-Sugui, Jr.: 0000-0002-3277-775X

Luis Ghivelder: 0000-0002-5667-6531

Present Address

S.S.: Department of Physics, Simon Fraser University, Burnaby, British Columbia, Canada V5A 1S6.

Notes

The authors declare no competing financial interest.

ACKNOWLEDGMENTS

S.S. acknowledges a postdoctoral fellowship from FAPERJ (Rio de Janeiro, Brazil), processo: E-26/202.848/2016. S.S.S. and L.G. are supported by CNPq and FAPERJ. L.F.C. is funded by The Leverhulme Trust Grant RPG-2016-306. The work at IOP, CAS is supported by the National Natural Science Foundation of China (11374011 and 11674372), the Strategic Priority Research Program (B) of the Chinese Academy of Sciences (CAS) (XDB07020300 and XDB25000000), and the Youth Innovation Promotion Association of CAS (2016004).

REFERENCES

(1) Kim, Y. B.; Hempstead, C. F.; Strnad, A. R. Critical Persistent Currents in Hard Superconductors. *Phys. Rev. Lett.* **1962**, *9*, 306.

(2) Anderson, P. W. Theory of Flux Creep in Hard Superconductors. *Phys. Rev. Lett.* **1962**, *9*, 309.

(3) Beasley, M. R.; Labusch, R.; Webb, W. W. Flux Creep in Type-II Superconductors. *Phys. Rev.* **1969**, *181*, 682. and references therein.

(4) Yeshurun, Y.; Malozemoff, A. P. Giant Flux Creep and Irreversibility in an YBaCuO Crystal: An Alternative to the Superconducting-Glass Model. *Phys. Rev. Lett.* **1988**, *60*, 2202.

(5) Abulafia, Y.; Shaulov, A.; Wolfus, Y.; Prozorov, R.; Burlachkov, L.; Yeshurun, Y.; Majer, D.; Zeldov, E.; Wühl, H.; Geshkenbein, V. B.; Vinokur, V. M. Plastic Vortex Creep in $YBa_2Cu_3O_{7-x}$ Crystals. *Phys. Rev. Lett.* **1996**, *77*, 1596.

(6) Rosenstein, B.; Shapiro, B. Y.; Shapiro, I.; Bruckental, Y.; Shaulov, A.; Yeshurun, Y. Peak Effect and Square-to-Rhombic Vortex Lattice Transition in $La_{7-x}Sr_xCuO_4$. *Phys. Rev. B: Condens. Matter Mater. Phys.* **2005**, *72*, 144512.

(7) Rosenstein, B.; Li, D. Ginzburg-Landau Theory of Type-II Superconductors in Magnetic Field. *Rev. Mod. Phys.* **2010**, *82*, 109.

(8) Rosenstein, B.; Zhuravlev, V. Quantitative Theory of Transport in Vortex Matter of Type-II Superconductors in the Presence of Random Pinning. *Phys. Rev. B: Condens. Matter Mater. Phys.* **2007**, *76*, 014507.

(9) Stamopoulos, D.; Speliotis, A.; Niarchos, D. From the Second Magnetization Peak to Peak Effect. A Study of Superconducting Properties in Nb Films and MgB_2 Bulk Samples. *Supercond. Sci. Technol.* **2004**, *17*, 1261.

(10) Kamihara, Y.; Watanabe, T.; Hirano, M.; Hosono, H. Iron-Based Layered Superconductor $La[O_{1-x}F_x]FeAs$ (x = 0.05−0.12) with T_c = 26 K. *J. Am. Chem. Soc.* **2008**, *130*, 3296.

(11) Hsu, F.-C.; Luo, J.-Y.; Yeh, K.-W.; Chen, T.-K.; Huang, T.-W.; Wu, P. W.; Lee, Y.-C.; Huang, Y.-L.; Chu, Y.-Y.; Yan, D.-C.; Wu, M.-K. Superconductivity in the PbO-type Structure α-FeSe. *Proc. Natl. Acad. Sci. U. S. A.* **2008**, *105*, 14262.

(12) Wen, H.-H.; Mu, G.; Fang, L.; Yang, H.; Zhu, X. Superconductivity at 25 K in Hole-Doped $(La_{1-x}Sr_x)OFeAs$. *Europhys. Lett.* **2008**, *82*, 17009.

(13) Ren, Z.-A.; Yang, J.; Lu, W.; Yi, W.; Shen, X.-L.; Li, Z.-C.; Che, G.-C.; Dong, X.-L.; Sun, L.-L.; Zhou, F.; Zhao, Z.-X. Superconductivity in the Iron-Based F-doped Layered Quaternary Compound $Nd[O_{1-x}F_x]FeAs$. *Europhys. Lett.* **2008**, *82*, 57002.

(14) Stewart, G. R. Superconductivity in Iron Compounds. *Rev. Mod. Phys.* **2011**, *83*, 1589.

(15) Senatore, C.; Flükiger, R.; Cantoni, M.; Wu, G.; Liu, R. H.; Chen, X. H. Upper Critical Fields Well Above 100 T for the Superconductor $SmFeAsO_{0.85}F_{0.15}$ with T_c = 46 K. *Phys. Rev. B: Condens. Matter Mater. Phys.* **2008**, *78*, 054514.

(16) Jaroszynski, J.; Hunte, F.; Balicas, L.; Jo, Y. J.; Raičević, I.; Gurevich, A.; Larbalestier, D. C.; Balakirev, F. F.; Fang, L.; Cheng, P.; Jia, Y.; Wen, H.-H. Upper Critical Fields and Thermally-Activated Transport of $NdFeAsO_{0.7}F_{0.3}$ Single Crystal. *Phys. Rev. B: Condens. Matter Mater. Phys.* **2008**, *78*, 174523.

(17) Wang, Z.; Xie, T.; Kampert, E.; Förster, T.; Lu, X.; Zhang, R.; Gong, D.; Li, S.; Herrmannsdörfer, T.; Wosnitza, J.; Luo, H. Electron Doping Dependence of the Anisotropic Superconductivity in $BaFe_{2-x}Ni_xAs_2$. *Phys. Rev. B: Condens. Matter Mater. Phys.* **2015**, *92*, 174509.

(18) Yuan, H. Q.; Singleton, J.; Balakirev, F. F.; Baily, S. A.; Chen, G. F.; Luo, J. L.; Wang, N. L. Nearly Isotropic Superconductivity in $(Ba,K)Fe_2As_2$. *Nature (London, U. K.)* **2009**, *457*, 565.

(19) Altarawneh, M. M.; Collar, K.; Mielke, C. H.; Ni, N.; BudâĂŹko, S. L.; Canfield, P. C. Determination of Anisotropic H_{c2} up to 60 T in $Ba_{0.55}K_{0.45}Fe_2As_2$ Single Crystals. *Phys. Rev. B* **2008**, *78*, No. 220505(R).

(20) Katase, T.; Ishimaru, Y.; Tsukamoto, A.; Hiramatsu, H.; Kamiya, T.; Tanabe, K.; Hosono, H. Advantageous Grain Boundaries in Iron Pnictide Superconductors. *Nat. Commun.* **2011**, *2*, 409.

(21) Durrell, J. H.; Eom, C.-B.; Gurevich, A.; Hellstrom, E. E.; Tarantini, C.; Yamamoto, A.; Larbalestier, D. C. The Behavior of Grain Boundaries in the Fe-based Superconductors. *Rep. Prog. Phys.* **2011**, *74*, 124511.

DOI: 10.1021/acsaelm.8b00014
ACS Appl. Electron. Mater. 2019, 1, 179−188

(22) Hosono, H.; Yamamoto, A.; Hiramatsu, H.; Ma, Y. Recent Advances in Iron-based Superconductors Toward Applications. *Mater. Today* **2018**, *21*, 278.
(23) Thuneberg, E. V.; Kurkijärvi, J.; Rainer, D. Pinning of a Vortex Line to a Small Defect in Superconductors. *Phys. Rev. Lett.* **1982**, *48*, 1853.
(24) Prozorov, R.; Ni, N.; Tanatar, M. A.; Kogan, V. G.; Gordon, R. T.; Martin, C.; Blomberg, C.; Prommapan, P.; Yan, J. Q.; Bud'ko, S. L.; Canfield, P. C. Vortex Phase Diagram of $Ba(Fe_{0.93}Co_{0.07})_2As_2$ Single Crystals. *Phys. Rev. B: Condens. Matter Mater. Phys.* **2008**, *78*, 224506.
(25) Kopeliansky, R.; Shaulov, A.; Shapiro, B. Y.; Yeshurun, Y.; Rosenstein, B.; Tu, J. J.; Li, L. J.; Cao, G. H.; Xu, Z. A. Possibility of Vortex Lattice Structural Phase Transition in the Superconducting Pnictide $Ba(Fe_{0.925}Co_{0.075})_2As_2$. *Phys. Rev. B: Condens. Matter Mater. Phys.* **2010**, *81*, 092504.
(26) Li, L. J.; Nishio, T.; Xu, Z. A.; Moshchalkov, V. V. Low-field Vortex Patterns in the Multiband $BaFe_{2-x}Ni_xAs_2$ Superconductor (x = 0.1, 0.16). *Phys. Rev. B: Condens. Matter Mater. Phys.* **2011**, *83*, 224522.
(27) Miu, D.; Noji, T.; Adachi, T.; Koike, Y.; Miu, L. On the Nature of the Second Magnetization Peak in $FeSe_{1-x}Te_x$ Single Crystals. *Supercond. Sci. Technol.* **2012**, *25*, 115009.
(28) Pervakov, K. S.; Vlasenko, V. A.; Khlybov, E. P.; Zaleski, A.; Pudalov, V. M.; Eltsev, Y. F. Bulk Magnetization and Strong Intrinsic Pinning in Ni-Doped $BaFe_2As_2$ Single Crystals. *Supercond. Sci. Technol.* **2013**, *26*, 015008.
(29) Su, T. S.; Yin, Y. W.; Teng, M. L.; Zhang, M. J.; Li, X. G. Angular Dependence of Vortex Dynamics in $BaFe_{1.9}Ni_{0.1}As_2$ Single Crystal. *Mater. Res. Express* **2014**, *1*, 016003.
(30) Sundar, S.; Salem-Sugui, S., Jr.; Amorim, H. S.; Wen, H.-H.; Yates, K. A.; Cohen, L. F.; Ghivelder, L. Plastic Pinning Replaces Collective Pinning as the Second Magnetization Peak Disappears in the Pnictide Superconductor $Ba_{0.75}K_{0.25}Fe_2As_2$. *Phys. Rev. B: Condens. Matter Mater. Phys.* **2017**, *95*, 134509.
(31) Liu, Y.; Zhou, L.; Sun, K.; Straszheim, W. E.; Tanatar, M. A.; Prozorov, R.; Lograsso, T. A. Doping Evolution of the Second Magnetization Peak and Magnetic Relaxation in $(Ba_{1-x}K_x)Fe_2As_2$ Single Crystals. *Phys. Rev. B: Condens. Matter Mater. Phys.* **2018**, *97*, 054511.
(32) Sundar, S.; Mosqueira, J.; Alvarenga, A. D.; Sóñora, D.; Sefat, A. S.; Salem-Sugui, S., Jr. Study of the Second Magnetization Peak and the Pinning Behaviour in $Ba(Fe_{0.935}Co_{0.065})_2As_2$ Pnictide Superconductor. *Supercond. Sci. Technol.* **2017**, *30*, 125007.
(33) Zhou, W.; Xing, X.; Wu, W.; Zhao, H.; Shi, Z. Second Magnetization Peak Effect, Vortex Dynamics, and Flux Pinning in 112-Type Superconductor $Ca_{0.8}La_{0.2}Fe_{1-x}Co_xAs_2$. *Sci. Rep.* **2016**, *6*, 22278.
(34) Hecher, J.; Zehetmayer, M.; Weber, H. W. How the Macroscopic Current Correlates with the Microscopic Flux-line Distribution in a type-II Superconductor: An Experimental Study. *Supercond. Sci. Technol.* **2014**, *27*, 075004.
(35) Pramanik, A. K.; Harnagea, L.; Nacke, C.; Wolter, A. U. B.; Wurmehl, S.; Kataev, V.; Büchner, B. Fishtail Effect and Vortex Dynamics in LiFeAs Single Crystals. *Phys. Rev. B: Condens. Matter Mater. Phys.* **2011**, *83*, 094502.
(36) Salem-Sugui, S., Jr.; Ghivelder, L.; Alvarenga, A. D.; Cohen, L. F.; Luo, H.; Lu, X. Fishtail and Vortex Dynamics in the Ni-doped Iron Pnictide $BaFe_{1.82}Ni_{0.18}As_2$. *Phys. Rev. B: Condens. Matter Mater. Phys.* **2011**, *84*, 052510.
(37) Salem-Sugui, S., Jr.; Ghivelder, L.; Alvarenga, A. D.; Cohen, L. F.; Luo, H.; Lu, X. Vortex Dynamics as a Function of Field Orientation in $BaFe_{1.9}Ni_{0.1}As_2$. *Supercond. Sci. Technol.* **2013**, *26*, 025006.
(38) Ahmad, D.; Choi, W. J.; Seo, Y. I.; Jung, S. G.; Kim, Y. C.; Salem-Sugui, S., Jr.; Park, T.; Kwon, Y. S. Doping Dependence of the Vortex Dynamics in Single Crystal Superconducting $NaFe_{1-x}Co_xAs$. *Supercond. Sci. Technol.* **2017**, *30*, 105006.
(39) Maley, M. P.; Willis, J. O.; Lessure, H.; McHenry, M. E. Dependence of Flux-Creep Activation Energy Upon Current Density in Grain-aligned $YBa_2Cu_3O_{7-x}$. *Phys. Rev. B: Condens. Matter Mater. Phys.* **1990**, *42*, No. 2639.
(40) Feigel'man, M. V.; Geshkenbein, V. B.; Larkin, A. I.; Vinokur, V. M. Theory of Collective Flux Creep. *Phys. Rev. Lett.* **1989**, *63*, 2303.
(41) Chen, Y.; Lu, X.; Wang, M.; Luo, H.; Li, S. Systematic Growth of $BaFe_{2-x}Ni_xAs_2$ Large Crystals. *Supercond. Sci. Technol.* **2011**, *24*, 065004.
(42) Perkins, G. K.; Moore, J.; Bugoslavsky, Y.; Cohen, L. F.; Jun, J.; Kazakov, S. M.; Karpinski, J.; Caplin, A. D. Superconducting Critical Fields and Anisotropy of a MgB_2 Single Crystal. *Supercond. Sci. Technol.* **2002**, *15*, 1156.
(43) Zhang, W.; Dai, Y.-M.; Xu, B.; Yang, R.; Liu, J.-Y.; Sui, Q.-T.; Luo, H.-Q.; Zhang, R.; Lu, X.-Y.; Yang, H.; Qiu, X.-G. Magnetoresistivity and Filamentary Superconductivity in Nickel-Doped $BaFe_2As_2$. *Chin. Phys. B* **2016**, *25*, 047401.
(44) Wang, M.; Luo, H.; Zhao, J.; Zhang, C.; Wang, M.; Marty, K.; Chi, S.; Lynn, J. W.; Schneidewind, A.; Li, S.; Dai, P. Electron-Doping Evolution of the Low-Energy Spin Excitations in the Iron Arsenide Superconductor $BaFe_{2-x}Ni_xAs_2$. *Phys. Rev. B: Condens. Matter Mater. Phys.* **2010**, *81*, 174524.
(45) Yeshurun, Y.; Burlachkov, N. B. L.; Kapitulnik, A. Dynamic Characteristics of the Anomalous Second Peak in the Magnetization Curves of Bi-Sr-Ca-Cu-O. *Phys. Rev. B: Condens. Matter Mater. Phys.* **1994**, *49*, 1548.
(46) Tamegai, T.; Iye, Y.; Oguro, I.; Kishio, K. Anomalous Peak Effect in Single Crystal $Bi_2Sr_2CaCu_2O_{8+y}$ Studied by Hall Probe Magnetometry. *Phys. C* **1993**, *213*, 33.
(47) Brown, S. P.; Charalambous, D.; Jones, E. C.; Forgan, E. M.; Kealey, P. G.; Erb, A.; Kohlbrecher, J. Triangular to Square Flux Lattice Phase Transition in $YBa_2Cu_3O_7$. *Phys. Rev. Lett.* **2004**, *92*, 067004.
(48) Taen, T.; Nakajima, Y.; Tamegai, T.; Kitamura, H. Enhancement of Critical Current Density and Vortex Activation Energy in Proton-Irradiated Co-Doped $BaFe_2As_2$. *Phys. Rev. B: Condens. Matter Mater. Phys.* **2012**, *86*, 094527.
(49) Griessen, R.; Hoekstra, A. F. T.; Wen, H.-H.; Doornbos, G.; Schnack, H. G. Negative-μ Vortex Dynamics in High-T_c Superconducting Films. *Phys. C* **1997**, *282*−*287*, 347.
(50) Salem-Sugui, S., Jr.; Ghivelder, L.; Alvarenga, A. D.; Cohen, L. F.; Yates, K. A.; Morrison, K.; Pimentel, J. L., Jr.; Luo, H.; Wang, Z.; Wen, H.-H. Flux Dynamics Associated with the Second Magnetization Peak in the Iron Pnictide $Ba_{1-x}K_xFe_2As_2$. *Phys. Rev. B: Condens. Matter Mater. Phys.* **2010**, *82*, 054513.
(51) Sun, Y.; Taen, T.; Tsuchiya, Y.; Pyon, S.; Shi, Z.; Tamegai, T. Magnetic Relaxation and Collective Vortex Creep in $FeTe_{0.6}Se_{0.4}$ Single Crystal. *Europhys. Lett.* **2013**, *103*, 57013.
(52) Haberkorn, N.; Miura, M.; Maiorov, B.; Chen, G. F.; Yu, W.; Civale, L. Strong Pinning and Elastic to Plastic Vortex Crossover in Na-doped $CaFe_2As_2$ Single Crystals. *Phys. Rev. B: Condens. Matter Mater. Phys.* **2011**, *84*, 094522.
(53) McHenry, M. E.; Simizu, S.; Lessure, H.; Maley, M. P.; Coulter, J. Y.; Tanaka, I.; Kojima, H. Dependence of the Flux-creep Activation Energy on the Magnetization Current for a $La_{1.86}Sr_{0.14}CuO_4$ Single Crystal. *Phys. Rev. B: Condens. Matter Mater. Phys.* **1991**, *44*, 7614.
(54) Bean, C. P. Magnetization of High-Field Superconductors. *Rev. Mod. Phys.* **1964**, *36*, 31.
(55) Song, D.; Ishida, S.; Iyo, A.; Nakajima, M.; Shimoyama, J. I.; Eisterer, M.; Eisaki, H. Distinct Doping Dependence of Critical Temperature and Critical Current Density in $Ba_{1-x}K_xFe_2As_2$ Superconductor. *Sci. Rep.* **2016**, *6*, 26671.
(56) Pallecchi, I.; Eisterer, M.; Malagoli, A.; Putti, M. Application Potential of Fe-Based Superconductors. *Supercond. Sci. Technol.* **2015**, *28*, 114005.
(57) Shahbazi, M.; Wang, X. L.; Choi, K. Y.; Dou, S. X. Flux Pinning Mechanism in $BaFe_{1.9}Ni_{0.1}As_2$ Single Crystals: Evidence for

DOI: 10.1021/acsaelm.8b00014
ACS Appl. Electron. Mater. 2019, 1, 179−188

Fluctuation in Mean Free Path Induced Pinning. *Appl. Phys. Lett.* **2013**, *103*, 032605.
(58) Sun, D. L.; Liu, Y.; Lin, C. T. Comparative Study of Upper Critical Field H_{c2} and Second Magnetization Peak H_{sp} in Hole and Electron-Doped $BaFe_2As_2$ Superconductor. *Phys. Rev. B: Condens. Matter Mater. Phys.* **2009**, *80*, 144515.
(59) Dew-Hughes, D. Flux Pinning Mechanisms in Type-II Superconductors. *Philos. Mag.* **1974**, *30*, 293.
(60) Koblischka, M. R.; van Dalen, A. J. J.; Higuchi, T.; Yoo, S. I.; Murakami, M. Analysis of Pinning in $NdBa_2Cu_3O_{7-\delta}$ Superconductors. *Phys. Rev. B: Condens. Matter Mater. Phys.* **1998**, *58*, 2863.
(61) Matin, Md.; Sharath Chandra, L. S.; Chattopadhyay, M. K.; Meena, R. K.; Kaul, R.; Singh, M. N.; Sinha, A. K.; Roy, S. B. Magnetic Irreversibility and Pinning Force Density in the Ti-V Alloys. *J. Appl. Phys.* **2013**, *113*, 163903.
(62) Koblischka, M. R.; Muralidhar, M. Pinning Force Scaling Analysis of Fe-based High-T_c Superconductors. *Int. J. Mod. Phys. B* **2016**, *30*, 1630017.
(63) Griessen, R.; Wen, H.-H.; van Dalen, A. J. J.; Dam, B.; Rector, J.; Schnack, H. G.; et al. Evidence for Mean Free Path Fluctuation Induced Pinning in $YBa_2Cu_3O_7$ and $YBa_2Cu_4O_8$ Films. *Phys. Rev. Lett.* **1994**, *72*, 1910.
(64) Vlasenko, V. A.; Pervakov, K. S.; Gavrilkin, S. Y.; Eltsev, Y. F. Unconventional Pinning in Iron Based Superconductors of 122 Family. *Phys. Procedia* **2015**, *67*, 952−957.
(65) Ghorbani, S. R.; Wang, X.-L.; Hossain, M. S. A.; Yao, Q. W.; Dou, S. X.; Lee, S. I.; Chung, K. C.; Kim, Y. K. Strong Competition Between the δl and δT_c Flux Pinning Mechanisms in MgB_2 Doped with Carbon Containing Compounds. *J. Appl. Phys.* **2010**, *107*, 113921.

DOI: 10.1021/acsaelm.8b00014
ACS Appl. Electron. Mater. 2019, 1, 179−188